Correction for Oral Contrast Artifacts in CT Attenuation-Corrected PET Images Obtained by Combined PET/CT

Sadek A. Nehmeh, PhD[1]; Yusuf E. Erdi, DSc[1]; Hovanes Kalaigian, MS[1]; Katherine S. Kolbert, MS[1]; Tinsu Pan, PhD[2]; Henry Yeung, MD[3]; Olivia Squire, BA[3]; Arvind Sinha, MD[3]; Steve M. Larson, MD[3]; and John L. Humm, PhD[1]

[1]Department of Medical Physics, Memorial Sloan-Kettering Cancer Center, New York, New York; [2]Applied Science Laboratory, General Electric Medical Systems, Waukesha, Wisconsin; and [3]Nuclear Medicine Service, Department of Radiology, Memorial Sloan-Kettering Cancer Center, New York, New York

Recent studies have shown increased artifacts in CT attenuation-corrected (CTAC) PET images acquired with oral contrast agents because of misclassification of contrast as bone. We have developed an algorithm, segmented contrast correction (SCC), to properly transform CT numbers in the contrast regions from CT energies (40–140 keV) to PET energy at 511 keV. **Methods:** A bilinear transformation, equivalent to that supplied by the PET/CT scanner manufacturer, for the conversion of linear attenuation coefficients of normal tissues from CT to PET energies was optimized for $BaSO_4$ contrast agent. This transformation was validated by comparison with the linear attenuation coefficients measured for $BaSO_4$ at concentrations ranging from 0% to 80% at 511 keV for PET transmission images acquired with ^{68}Ge rod sources. In the CT images, the contrast regions were contoured to exclude bony structures and then segmented on the basis of a minimum threshold CT number (300 Hounsfield units). The CT number in each pixel identified with contrast was transformed into the corresponding effective bone CT number to produce the correct attenuation coefficient when the data were translated by the manufacturer software into PET energy during the process of CT attenuation correction. CT images were then used for attenuation correction of PET emission data. The algorithm was validated with a phantom in which a lesion was simulated within a volume of $BaSO_4$ contrast and in the presence of a human vertebral bony structure. Regions of interest in the lesion, bone, and contrast on emission PET images reconstructed with and without the SCC algorithm were analyzed. The results were compared with those for images obtained with ^{68}Ge-based transmission attenuation-corrected PET. **Results:** The SCC algorithm was able to correct for contrast artifacts in CTAC PET images. In the phantom studies, the use of SCC resulted in an approximate 32% reduction in the apparent activity concentration in the lesion compared with data obtained from PET images without SCC and a $<$7.6% reduction compared with data obtained from ^{68}Ge-based attenuation-corrected PET images. In one clinical study, maximum standardized uptake value (SUV_{max}) measurements for the lesion, bladder, and bowel were, respectively, 14.52, 13.63, and 13.34 g/mL in CTAC PET images, 59.45, 26.71, and 37.22 g/mL in ^{68}Ge-based attenuation-corrected PET images, and 11.05, 6.66, and 6.33 g/mL in CTAC PET images with SCC. **Conclusion:** Correction of oral contrast artifacts in PET images obtained by combined PET/CT yielded more accurate quantitation of the lesion and other, normal structures. The algorithm was tested in a clinical case, in which SUV_{max} measurements showed discrepancies of 2%, 1.3%, and 5% between ^{68}Ge-based attenuation-corrected PET images and CTAC PET images with SCC for the lesion, bladder, and bowel, respectively. These values correspond to 6.5%, 62%, and 66% differences between CTAC-based measurements and ^{68}Ge-based ones.

Key Words: PET/CT contrast artifacts

J Nucl Med 2003; 44:1940–1944

In most CT examinations that include the abdomen or the pelvis, oral contrast agent usually is administered. Oral contrast agent allows more accurate identification of the bowel and facilitates the interpretation of abdominal and pelvic CT studies (*1*–*3*). In PET/CT studies, oral contrast agent also would improve image quality, resulting in an increase in diagnostic capacity (*4*,*5*). However, the use of oral contrast agent or the presence of any high-atomic-number material, such as a metallic implant (*6*), might induce artifacts in CT attenuation-corrected (CTAC) PET images (*7*). The high atomic numbers of contrast agents result in an increased fraction of photoelectric interactions in regions of contrast accumulation, yielding increased Hounsfield units (HU) or CT numbers. CT numbers for regions of contrast can range from a few HU to 3,071 HU (maximum CT number), depending on the contrast agent concentration. As a result, and with the current available algorithms, contrast can be misclassified as high-density bone and thus can be associated with an incorrect scaling factor. Consequently, the 511-keV-equivalent attenuation coefficient values for contrast are overestimated, resulting in overcorrection for attenuation in PET images and consequently in overestimation of the apparent reconstructed

Received Mar. 27, 2003; revision accepted Aug. 28, 2003.

For correspondence or reprints contact: Sadek A. Nehmeh, PhD, Department of Medical Physics, Memorial Sloan-Kettering Cancer Center, 1275 York Ave., New York, NY 10021.

E-mail: nehmehs@mskcc.org

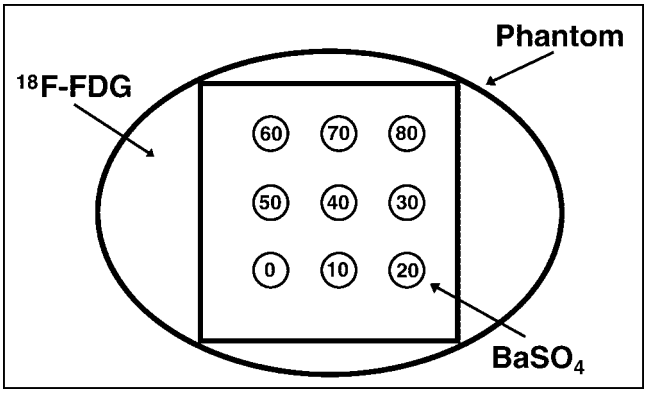

FIGURE 1. Drawing of transaxial cross-section of phantom 1, with 9 syringes fixed in Styrofoam (The Dow Chemical Co.) sheet and filled with $BaSO_4$ contrast agent at concentrations of 0%–80% (represented by numbers in circles that represent syringes).

activity concentration of the radiotracer in the contrast region. When a lesion is present within the contrast volume, the above-mentioned artifact will result in an overestimation of the lesion standardized uptake value (SUV).

In this study, we propose a method to correct for contrast artifacts in CTAC PET images. This method is performed by contouring the contrast regions, excluding any bony structures; transforming the corresponding linear attenuation coefficients, $\mu(\mathbf{x},E)$, of contrast correctly from CT to PET energies; and, finally, reconstructing CTAC PET images with the appropriately scaled attenuation map. In this article, we present the initial evaluation of this method in 2 phantom studies and 1 clinical case.

MATERIALS AND METHODS

PET/CT Scanner

Data referenced in this study were acquired with a Discovery LS PET (Advance NXi)/CT (LightSpeed 4-slice) scanner (GE Medical Systems). The LightSpeed CT scanner has a 50-cm transaxial field of view (FOV) and is able to acquire images with a slice thickness ranging from 1.25 to 20.0 mm. The tube current can be varied between 10 and 440 mA, and the tube voltage settings are 80, 100, 120, and 140 KVp. The table feed rate of the CT scanner ranges from 1.25 to 30 mm per 360° rotation of the x-ray tube. The maximum scan time in the helical acquisition mode is 120 s, and the spatial resolution is 0.32 mm.

The Advance NXi PET scanner is a whole-body scanner with a transaxial FOV of 55 cm and a 14.75-cm FOV along the axial direction. The scanner contains retractable septa and can be used in the 2-dimensional mode (septa extended) for high-resolution imaging or in the 3-dimensional mode (septa retracted) for a higher sensitivity (1,200 kcps/mCi/mL). The image resolution is 4.2 mm in full width at half maximum. All measurements performed in this study were acquired in the 2-dimensional mode.

Phantoms

Phantom 1 consisted of nine 30-mL syringes filled with $BaSO_4$ contrast agent at concentrations of 1.3%, 5%, 10%, 20%, 30%, 40%, 50%, 60%, and 80%. The syringes were immersed in a background of ^{18}F-FDG at 37×10^3 Bq/mL (Fig. 1). No ^{18}F-FDG was added to the syringes, which therefore should register zero activity by analysis of regions of interest (ROI).

Phantom 2 consisted of one 30-mL syringe filled with ^{18}F-FDG (to simulate a lesion) and placed in a bottle of $BaSO_4$ contrast agent (50%, w/w). This bottle was fixed within a larger phantom shell containing a background of ^{18}F-FDG at 37×10^3 Bq/mL. Also contained within the phantom shell and immersed in the background was a human vertebra to test the effect of correcting contrast artifacts on bone (Fig. 2). The ratio of lesion activity to background activity was 3:1.

Patient Data

This study included one 45-y-old male patient diagnosed with rectal carcinoma. The patient underwent a helical CT scan for attenuation correction and then a 4-min-per-bed-position PET emission study. A conventional transmission PET scan performed with ^{68}Ge rod sources also was acquired as a gold standard. Before the PET/CT studies, the patient underwent conventional simulation studies for radiotherapy planning purpose. The patient was given ~240 mL of diluted $BaSO_4$ contrast agent (50% concentration) orally and 15 mL of 98% concentrated $BaSO_4$ (liquid Polibar; E-Z-EM Canada Inc.), followed by 15 mL of air, both administered in an enema.

Data Acquisition

In all studies, a helical CT scan, a 4-min-per-bed-position emission scan, and a 3-min-per-bed-position transmission scan with a ^{68}Ge rod source were performed. PET emission data, in accordance with our standard clinical protocol, were corrected for attenuation with both CT and ^{68}Ge by use of the image-reconstruction-with-segmented-attenuation-correction (IRSAC) algorithm. The helical CT scan was performed at 80 mA and 140 KVp.

Transformation of $\mu(x,E)$ from 80 keV to 511 keV

The effective CT energy of our Discovery LS PET/CT scanner was measured to be 80 keV (data not shown). The conversion of $\mu(\mathbf{x},E)$ from CT energies to PET energy by the Discovery LS software consists of an initial rebinning of the CT images, acquired at 512×512 matrices, to 128×128, to match the PET pixel resolution. Subsequently, the CT values are transformed to

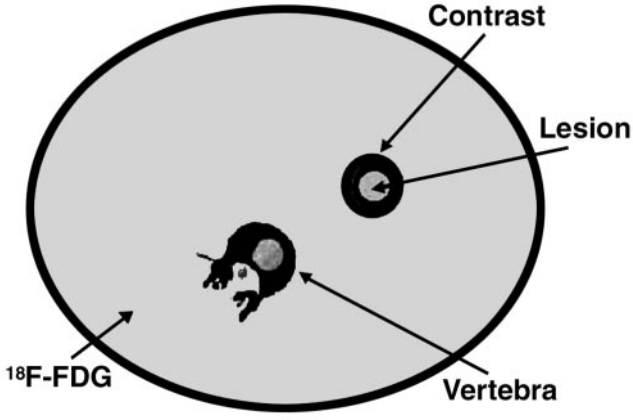

FIGURE 2. Transaxial CT image of phantom 2, with shell filled with ^{18}F-FDG and containing simulated lesion inside bottle of $BaSO_4$ contrast agent and human vertebra.

511-keV energy as follows (*2*):

$$\mu^{PET}|CT < 0 = \mu^{PET}_{H_2O}(CT + 1{,}000)/1{,}000 \quad CT < 0 \qquad \text{Eq. 1}$$

$$\mu^{PET}|CT > 0 = \mu^{PET}_{H_2O} + CT[\mu^{CT}_{H_2O}/1{,}000(\mu^{CT}_{Bone} - \mu^{CT}_{H_2O})] \times (\mu^{PET}_{Bone} - \mu^{PET}_{H_2O}) \quad CT > 0, \qquad \text{Eq. 2}$$

where μ^{PET} is the linear attenuation coefficient at PET energy (511 keV), CT is the CT number, and μ^{PET}_{Bone}, $\mu^{PET}_{H_2O}$, μ^{CT}_{Bone}, and $\mu^{CT}_{H_2O}$ are the linear attenuation coefficients for bone and water at the corresponding equivalent CT (80 keV) and PET energies. These coefficients are calculated from the tables of Berger et al. (*8*) for monochromatic energies and are 0.172, 0.096, 0.428, and 0.184 cm^{-1}, respectively.

The validity of the above transformation is based on the fact that human tissues have almost the same electron density as water. However, in the presence of a contrast agent, such as $BaSO_4$, Equation 2 should be modified as follows:

$$\mu^{PET}|CT > 150 = \mu^{PET}_{H_2O} + CT[\mu^{CT}_{H_2O}/1{,}000(\mu^{CT}_{BaSO_4} - \mu^{CT}_{H_2O})] \times (\mu^{PET}_{BaSO_4} - \mu^{PET}_{H_2O}), \qquad \text{Eq. 3}$$

where $\mu^{CT}_{BaSO_4}$ is 9.81750 cm^{-1} and $\mu^{PET}_{BaSO_4}$ is 0.37995 cm^{-1}.

Because of the maximum of 12 bits of allocated memory for CT numbers, any CT number above 3,071 HU is truncated. Figure 3 shows that a CT number of 3,071 HU is reached for a $BaSO_4$ concentration of 60%. Consequently, $\mu^{PET}_{BaSO_4}$ and $\mu^{CT}_{BaSO_4}$ in Equation 3 should correspond to such a concentration.

Analysis

In the first phantom study, ROIs were drawn manually for all 9 syringes in both the CTAT PET and the ^{68}Ge-based attenuation-corrected PET images. The maximum activity concentration within each ROI was measured by use of the software provided by the scanner manufacturer. Also, ROIs were drawn for all 9 syringes in the CT and ^{68}Ge transmission images.

In the second phantom study, the contrast region was segmented by drawing manually an ROI around it while excluding the vertebral structure.

In the clinical study, the contrast regions in all transaxial slices were also contoured manually, excluding any bony structures.

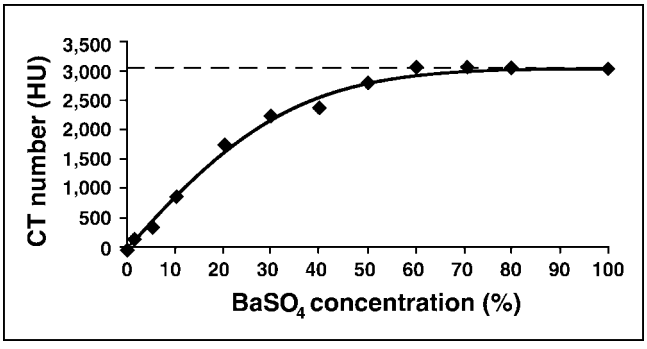

FIGURE 3. CT number in HU versus concentration of oral $BaSO_4$ contrast agent. As concentration of $BaSO_4$ increases, CT number reaches plateau at 3,071 HU because of maximum of 12 bits of allocated memory in CT.

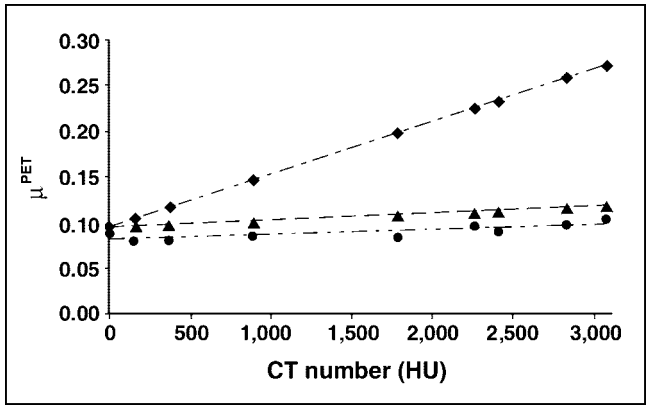

FIGURE 4. Linear attenuation coefficients at PET energy of 511 keV as function of CT number of $BaSO_4$ measured experimentally at different concentrations. Linear attenuation values calculated by Discovery LS algorithm (◆), optimized for human tissues, by transformation optimized for $BaSO_4$ contrast agent (▲), and by use of ^{68}Ge rod sources (●) are shown.

Transformation of μ(x,E) of $BaSO_4$ Contrast Agent from 80 keV to 511 keV

The μ(**x**,E) of $BaSO_4$ contrast agent needs to be transformed from 80 keV to 511 keV. However, the Discovery LS algorithm is intended to correct the linear attenuation coefficients of tissues (including bone), but not contrast. This issue can be solved as follows. First, contour the contrast, segmenting the contrast on the basis of a minimum CT number threshold of 150 HU, excluding any bony structures. This threshold, which corresponds to a $BaSO_4$ concentration of 1.3%, was deduced from our phantom measurements of the measured activity concentration in regions of different contrast agent concentrations (Fig. 2), with ^{68}Ge or CT data for attenuation correction. To contour (manually) the contrast regions, which were extracted as bitmaps (a matrix of values in which 1 represents a pixel within the contour and 0 represents a pixel elsewhere), we used the software package Multiple Image Analysis Utility (National Institutes of Health) (*9*). Second, substitute the CT value in each pixel within the contour and identified by the first threshold cut with the corresponding effective CT number for bone in Equations 1 and 2 to produce the correct μ(**x**,E) for $BaSO_4$ when the Discovery LS transformation (i.e., Equations 1 and 2) is applied. Then, having Equations 1 and 2 equal Equation 3 yields the effective bone CT number:

$$CT_{eff} = CT_{Bone}\left(\frac{\mu^{PET}_{BaSO_4} - \mu^{PET}_{H_2O}}{\mu^{CT}_{BaSO_4} - \mu^{CT}_{H_2O}}\right) \times \left(\frac{\mu^{CT}_{Bone} - \mu^{CT}_{H_2O}}{\mu^{PET}_{Bone} - \mu^{PET}_{H_2O}}\right),$$

where CT_{eff} is the effective CT number for bone that produces the correct μ^{PET} for $BaSO_4$, when converted from CT energy to PET energy using the PET/CT transformation algorithm, and CT is the CT number in each pixel within the contrast region, as measured by the PET/CT manufacturer software.

Attenuation Correction

The modified CT attenuation map was rebinned to match the PET pixel resolution, and then the CT values were transformed from 80 keV to 511 keV according to the Discovery LS algorithm and used for attenuation correction of the PET images.

TABLE 1

Area	SUV_{max} (g/mL) measured with attenuation correction: Rod source	CTAC	CTAC + SCC
Lesion	13.63	14.52	13.34
Bladder	36.71	59.45	37.22
Bowel	6.66	11.05	6.33

RESULTS

The modified transformation to estimate the linear attenuation coefficients, $\mu(\mathbf{x},E)$, at the PET energy (511 keV) for $BaSO_4$ contrast agent was validated by comparison with the ^{68}Ge rod source–based measurements at different $BaSO_4$ concentrations. Figure 4 shows a discrepancy between the calculated and the measured (with ^{68}Ge rod source) μ^{PET} values, with a χ^2 of 3.4%.

Measurements of the activity concentration in the simulated lesion of the second phantom in PET images reconstructed with and without segmented contrast correction (SCC) were within 7.6% and 32%, respectively, of the ^{68}Ge rod source-based attenuation correction.

In the clinical study, reconstruction of the PET images with SCC and the IRSAC algorithm resulted in a more accurate quantitation of the ^{18}F-FDG uptake in the lesion, as well as in other normal structures, relative to the gold standard values obtained with ^{68}Ge-based attenuation correction. Measurements of the maximum SUV (SUV_{max}) for the lesion, bladder, and bowel in PET images reconstructed with and without SCC and with ^{68}Ge-based attenuation correction are summarized in Table 1. Figure 5 shows sagittal views of the patient's lesion, bladder, and bowel in CTAC PET images, CTAC PET images with SCC, and ^{68}Ge-based attenuation-corrected PET images.

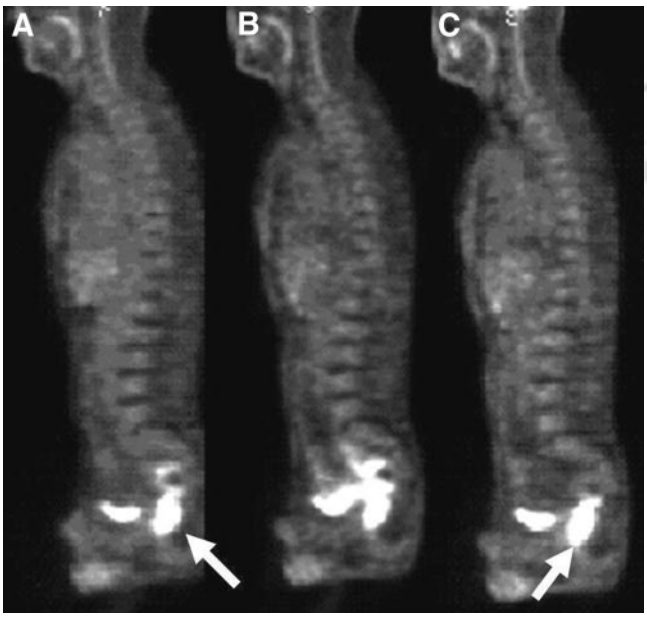

FIGURE 5. Patient's lesion as it appears in corresponding sagittal slices reconstructed with ^{68}Ge rod source–based attenuation correction (A), CTAC (B), and CTAC with SCC (C). Lesion is marked by arrows in panels A and C; it was not possible to determine extent of lesion in panel B because of uptake of contrast agent in bowel.

DISCUSSION

To exploit the advantages associated with combining CT and PET, clinical CT protocols, in particular, the use of oral contrast agents, must be fully implemented. The administration of oral contrast agents enables the delineation of intestinal structures from other retro- and intraperitoneal organs on CT (*4,10*), a factor that may improve accuracy in interpreting CT studies.

In PET imaging, intestinal ^{18}F-FDG uptake is commonly seen and may interfere with the diagnosis of malignant lesions (*4,11*). Dizendorf et al. (*4*) have reported on the advantage of using CT contrast agents to improve the coregistration of PET/CT. Although some studies have reported that slight artifacts, if any, are induced in CTAC PET images because of oral contrast agents (*4,12*), Antoch et al. (*5*) have shown the opposite for intravenous contrast agents. Contrast artifacts in PET images are related to the high atomic numbers of contrast agents relative to the atomic number of bone. As the concentration of a contrast agent increases, its corresponding CT number will fall within the CT number range for bone. Contrast will be misclassified as bone, and its linear attenuation coefficient, μ^{PET}, will be overestimated, leading to an overestimation of ^{18}F-FDG uptake. Figure 6 shows an increase in the measured activity in contrast agent–filled syringes of up to 6-fold when measured in CTAC PET images versus ^{68}Ge-based attenuated.

In this study, we have proposed a solution to more accurately quantitate lesion size and radiotracer uptake in

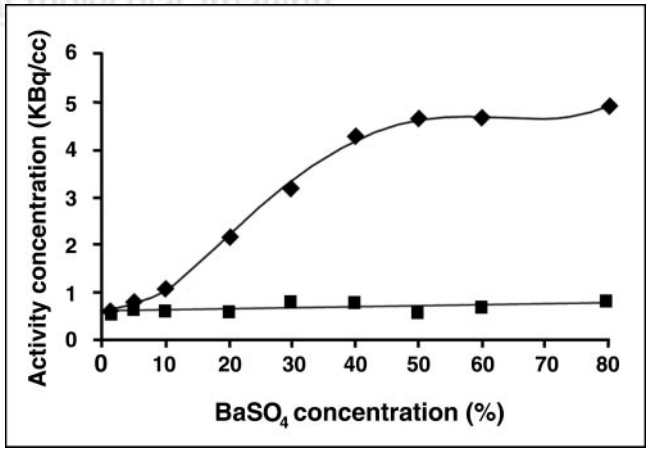

FIGURE 6. Measured activity concentration, reconstructed with CTAC, as function of concentration of $BaSO_4$ contrast agent (◆). Plateau is attained at high concentrations because of truncation of CT number. Readings measured with ^{68}Ge rod source–based attenuation correction are shown for comparison (■).

the presence of oral contrast agent. In this approach, we have proposed substituting the CT values for contrast agents with their equivalent effective bone CT numbers. The segmentation of contrast was based on a CT number of 150 HU, up to which no pronounced discrepancy in the measured activity concentrations between ^{68}Ge-based attenuation-corrected images and CTAC images has occurred. This fact is also in close agreement with what was reported by Cohade et al. (*13*). In Figure 4, a 19% discrepancy was measured between the bone (or $BaSO_4$) transformation-based μ^{PET} value of water at 511 keV and that measured with the ^{68}Ge rod sources. This finding suggests that the effective PET attenuation energy is lower than 511 keV, possibly because of a broadening in the detected transmission beam as a result of the broad energy window (300–650 keV) used to account for both the energy resolution of the PET detectors and the scatter in the patient (or phantom). Replacement of the narrow beam attenuation coefficient value of $\mu_{H_2O}^{PET}$ (0.096 cm^{-1}) with the experimental value (0.080192 cm^{-1}) reduced the discrepancy to 1.6%, in agreement with what was reported by Nakamoto et al. for water (*14*). As a result, the χ^2 was improved from 3.4% to 0.3%.

This method resulted in improved accuracy in the quantitation of ^{18}F-FDG. In phantom studies, a discrepancy of 7.6% in the SUV measurements between ^{68}Ge-based attenuation correction and CTAC with SCC was found. This result falls within the discrepancy range for ^{68}Ge-based attenuation-corrected PET images and CTAC PET images for normal organs, other than the lungs (1.6% for water and up to 11% for bone) (*14*). In the clinical evaluation, the SCC method resulted in a major improvement in accuracy in the quantitation of ^{18}F-FDG uptake in the lesion, bladder, and bowel. It also provided a more accurate definition of the lesion. In all measurements, the ^{68}Ge-based attenuation-corrected PET images were considered the gold standard. There were discrepancies of 2%, 1.3%, and 5% between the SUV_{max} measurements obtained by CTAC with SCC for the lesion, bladder, and bowel, respectively, and the ^{68}Ge-based measurements. These values correspond to 6.5%, 62%, and 66% differences between CTAC-based measurements and ^{68}Ge-based ones. The large discrepancies in the SUV_{max} for the bladder and bowel between ^{68}Ge-based measurements and CTAC-based ones are attributable to the high concentrations of oral contrast agents within the 2 volumes. For the lesion, which does not include any contrast, SUV_{max} measurements are consistent between the 2 attenuation correction methods. However, with SCC, the oral contrast artifact resulting in false reconstructed radiotracer uptake was totally eliminated.

Finally, this implementation of the SCC method does not account for the second-order effect of beam hardening of x-ray attenuation in regions of oral contrast. Such an artifact, in addition to degrading the quality of CT images, may affect accuracy in correcting for the attenuation effect in PET images. Hence, a correction method for the beam-hardening artifact may need to be developed.

CONCLUSION

A new method, SCC, has been developed to account for oral contrast artifacts in CTAC PET images obtained with a Discovery LS PET/CT scanner. The SCC method was evaluated in both phantom and clinical studies and enabled the accurate transformation of linear attenuation coefficients, $\mu(\mathbf{x},E)$, from CT energies to PET energy. This method resulted in accurate recovery of the lesion size and SUV measured in the ^{68}Ge-based attenuation-corrected PET images.

ACKNOWLEDGMENTS

The authors would like to thank all those who contributed to these promising results, in particular, Keith Pentlow, for all the valuable discussions and suggestions, and GE Medical Systems for providing the highest degree of cooperation.

REFERENCES

1. Megibow AJ, Bosniak MA. Dilute barium as a contrast agent for abdominal CT. *AJR*. 1980;34:1273–1274.
2. Burger C, Goerres GW, Schoenes S, Buck A, Lonn AHR, von Schulthess GK. PET attenuation coefficients from CT images: experimental evaluation of the transformation of CT into PET 511 keV attenuation coefficients. *Eur J Nucl Med*. 2002;29:922–927.
3. Garrett PR, Meshkov SL, Perlmutter GS. Oral contrast agents in CT of the abdomen. *Radiology*. 1984;153:545–546.
4. Dizendorf EV, Treyer V, Von Schulthess GK, Hany TF. Application of oral contrast media in coregistered positron emission tomography-CT. *AJR*. 2002; 179:477–481.
5. Antoch G, Freudenberg LS, Stattaus J, et al. Whole-body positron emission tomography-CT: optimized CT using oral and IV contrast materials. *AJR*. 2002; 179:1555–1560.
6. Goerres GW, Hany TF, Kamel EM, von Schulthess GK, Buck A. Head and neck imaging with PET and PET/CT: artifacts from dental metallic implants. *Eur J Nucl Med*. 2002;29:367–370.
7. Gerald A, Lutz SF, Thomas E, et al. Focal tracer uptake: a potential artifact in contrast-enhanced dual-modality PET/CT scans. *J Nucl Med*. 2002;43:1339–1342.
8. Berger MJ, Hubbell JH, Seltzer SM, Coursey JS, Zucker DS. XCOM: Photon Cross Sections Database [National Institute of Standards and Technology web site]. Available at: http://physics.nist.gov/PhysRefData/Xcom/Text/XCOM.html. Accessed October 17, 2003.
9. Kolbert KS, Hamacher KA, Jurcic JG, Scheinberg DA, Larson SM, Sgouros G. Parametric images of antibody pharmacokinetics in Bi213-HuM195 therapy of leukemia. *J Nucl Med*. 2001;42:27–32.
10. Hamlin DJ, Burgener FA. Positive and negative contrast agents in CT evaluation of the abdomen and pelvis. *J Comput Assist Tomogr*. 1981;5:82–90.
11. Jadvar H, Schambeye RB, Segall GM. Effect of atropine and sincalide on the intestinal uptake of F-18 fluorodeoxyglucose. *Clin Nucl Med*. 1999;24:965–967.
12. Kamel E, Hany TF, Burger C, et al. CT vs Ge-68 attenuation correction in a combined PET/CT system: evaluation of the effect of lowering the CT tube current. *Eur J Nucl Med Mol Imaging*. 2002;29:346–350.
13. Cohade C, Osman M, Nakamoto Y, et al. Initial experience with oral contrast in PET/CT: phantom and clinical studies. *J Nucl Med*. 2003;44:412–416.
14. Nakamoto Y, Osman M, Cohade C, et al. PET/CT: comparison of quantitative tracer uptake between germanium and CT transmission attenuation-corrected images. *J Nucl Med*. 2002;43:1137–1143.